Article

Current Biology

Connectomics-Based Analysis of Information Flow in the *Drosophila* Brain

Highlights

- A *Drosophila* connectome was reconstructed by 12,995 neuron images in FlyCircuit 1.1
- Hierarchical organization, small word, and rich club were observed in the brain
- Pathways of information flow during behavior were predicted from network structure
- Organization schemes of fly and mammalian brains showed fundamental similarities

Authors

Chi-Tin Shih, Olaf Sporns, ...,
Ralph J. Greenspan, Ann-Shyn Chiang

Correspondence

shih.chi.tin@gmail.com (C.-T.S.),
aschiang@life.nthu.edu.tw (A.-S.C.)

In Brief

A draft of the *Drosophila* connectome was reconstructed from 12,995 neuron images. The network showed hierarchical structure, small world, and rich-club organization. The present analysis revealed whole-brain patterns of network structure and rules of information flow. The overall organizational scheme showed fundamental similarities to the mammalian brain.

Shih et al., 2015, Current Biology *25*, 1–10
May 18, 2015
http://dx.doi.org/10.1016/j.cub.2015.03.021

CellPress

Please cite this article in press as: Shih et al., Connectomics-Based Analysis of Information Flow in the *Drosophila* Brain, Current Biology (2015), http://dx.doi.org/10.1016/j.cub.2015.03.021

Current Biology
Article

Connectomics-Based Analysis of Information Flow in the *Drosophila* Brain

Chi-Tin Shih,[1,*] Olaf Sporns,[2] Shou-Li Yuan,[3] Ta-Shun Su,[4] Yen-Jen Lin,[3] Chao-Chun Chuang,[5] Ting-Yuan Wang,[3] Chung-Chuang Lo,[4] Ralph J. Greenspan,[6] and Ann-Shyn Chiang[3,6,7,8,9,*]
[1]Department of Applied Physics, Tunghai University, Taichung 40704, Taiwan
[2]Department of Psychological and Brain Sciences, Indiana University, Bloomington, IN 47405, USA
[3]Brain Research Center, National Tsing Hua University, Hsinchu 30013, Taiwan
[4]Institute of Systems Neuroscience, National Tsing Hua University, Hsinchu 30013, Taiwan
[5]National Center for High-Performance Computing, Hsinchu 30076, Taiwan
[6]Kavli Institute for Brain and Mind, University of California, San Diego, La Jolla, CA 92093-0126, USA
[7]Institute of Biotechnology and Department of Life Science, National Tsing Hua University, Hsinchu 30013, Taiwan
[8]Department of Biomedical Science and Environmental Biology, Kaohsiung Medical University, Kaohsiung 80780, Taiwan
[9]Genomics Research Center, Academia Sinica, Nankang, Taipei 11529, Taiwan
*Correspondence: shih.chi.tin@gmail.com (C.-T.S.), aschiang@life.nthu.edu.tw (A.-S.C.)
http://dx.doi.org/10.1016/j.cub.2015.03.021

SUMMARY

Understanding the overall patterns of information flow within the brain has become a major goal of neuroscience. In the current study, we produced a first draft of the *Drosophila* connectome at the mesoscopic scale, reconstructed from 12,995 images of neuron projections collected in *FlyCircuit* (version 1.1). Neuron polarities were predicted according to morphological criteria, with nodes of the network corresponding to brain regions designated as local processing units (LPUs). The weight of each directed edge linking a pair of LPUs was determined by the number of neuron terminals that connected one LPU to the other. The resulting network showed hierarchical structure and small-world characteristics and consisted of five functional modules that corresponded to sensory modalities (olfactory, mechanoauditory, and two visual) and the pre-motor center. Rich-club organization was present in this network and involved LPUs in all sensory centers, and rich-club members formed a putative motor center of the brain. Major intra- and inter-modular loops were also identified that could play important roles for recurrent and reverberant information flow. The present analysis revealed whole-brain patterns of network structure and information flow. Additionally, we propose that the overall organizational scheme showed fundamental similarities to the network structure of the mammalian brain.

INTRODUCTION

Understanding the structural network of the brain—the connectome [1, 2]—is an essential step in understanding how the brain controls behavior and cognition [3]. Toward this goal, we used a database of 23,579 images of single neurons in the *Drosophila* brain, *FlyCircuit* version 1.1 (http://www.flycircuit.tw/v1.1) [4], to assemble a wiring diagram of the female *Drosophila* brain consisting of 12,995 projection neurons.

We previously proposed a criterion different from conventional anatomy to divide the brain into several functional units, including 43 local processing units (LPUs) and six interconnecting units [4]. An LPU is defined as having its own population of local interneurons (LNs) whose fibers are limited to that region and as delivering or receiving information via bundled neural tracts to or from other units. An interconnecting unit lacks its own population of LNs. Since LNs are presumed to be essential for information processing and modulation within the units, these interconnecting units appear to relay information to other LPUs unmodified by any local network interactions. For simplicity, "LPU" is used in the following text to represent all functional units in the brain discussed. The structure of the standard brain composed of LPUs is shown in Figure S1.

A comprehensive network of the synaptic connections between neurons is beyond the resolution of our confocal microscopy-based images. However, neuron-to-LPU connections can be determined accurately, and recent advances in morphological analyses of neuronal fibers have allowed for accurate predictions of the polarities of projection neurons [5–8], and hence the construction of a directed mesoscopic brain network. The weight of a link contributed by a single neuron between two LPUs, which were respectively innervated by dendrites and axons of the neuron, was set as the geometrical average of the number of dendritic and axonal terminals located in the two LPUs. The weight of each directed edge linking a LPU pair was the summation of the weight of all neurons that connected one LPU to the other in that direction (Figure S2). The resulting network was analyzed using methods from complex network theory.

RESULTS

FlyCircuit 1.1

The *FlyCircuit* database, a public resource for online archiving, cell type inventory, browsing, searching, analysis, and 3D visualization of individual neurons in the *Drosophila* brain [4], has been

Table 1. Numbers of Gal4 Neurons in the Standard Brain

Gal4 Driver (Neurotransmitter)	Total Gal4 Neurons in the Female Brain		Total Gal4 Neurons in the Male Brain	
	FlyCircuit	FlyCircuit 1.1	FlyCircuit	FlyCircuit 1.1
Cha-GAL4	2,348	3,377	0	0
fru-GAL4	1,454	2,758	2,055	3,378
G0239-GAL4	12	12	0	0
Gad1-GAL4	1,002	3,632	0	0
GH146-GAL4	1	1	6	6
npf-GAL4	41	159	41	200
Tdc2-GAL4	264	265	0	0
TH-GAL4	514	514	377	379
Trh-GAL4	989	995	1,186	1,188
VGlut-GAL4	5,867	6,005	0	0
5-HT1B-GAL4	41	41	57	58
E0585-GAL4	0	193	0	0
5-HT1A-GAL4	0	227	0	191

See also Tables S1 and S2.

updated to incorporate several new features: (1) additional image data of 23,579 neurons (Table 1), (2) assignment of axon/dendrite polarity for all individual neurons, and (3) transformed coordinates in a standard brain for all imaging data. Based on the assumption that major information is transmitted in a neuron from dendrite to axon, we used 12,995 projection neurons in the female brain collected in the *FlyCircuit* 1.1 to construct a network indicating directions of information flow among the various LPUs.

Basic Measurements

Strength, $\vec{s}$

The node strength for a weighted network was set as the summation of the weights of all edges connecting the node and its neighbors (Figure 1A). The dorsomedial protocerebrum (DMP), ventromedial protocerebrum (VMP), ventrolateral protocerebrum dorsal part (VLP-D), fanshaped body (FB), caudal ventrolateral protocerebrum (CVLP), and superior dorsofrontal protocerebrum (SDFP) were the strongest nodes.

Node Polarity, $\vec{p}$

Positive and negative values indicated "receivers" and "senders," respectively (Figure 1B). The protocerebral bridge (PB) in the central complex had the strongest sender characteristic, with a polarity of −0.87, and the first-layer sensory LPUs, like antennal lobes (AL) for olfaction [9] and antennal mechanosensory and motor center (AMMC) for hearing [10, 11], were also senders (negative polarity). AL sent signals to the lateral horn (LH) and mushroom bodies (MB), and AMMC sent to CVLP. Both AL and AMMC received signals from peripheral sensory neurons, not included in the present study, and also from their counterparts in the opposite hemisphere. Polarity for medulla (MED), the first-layer LPU for vision [12], was positive with VMP and CVLP, the strongest upstream LPUs, implying that MED has functions other than purely visual input, for example, the integration of visual and auditory signals.

Another heavily connected LPU FB in central complex had a moderately negative polarity of −0.265. The link from FB to inferior dorsofrontal protocerebrum (IDFP) was the strongest link in the whole network.

Downstream LPUs of strong senders, such as IDFP (downstream of FB and PB), LH, MB (downstream of AL), and lobula (LOB) (downstream of MED), naturally tended to be receivers. An exception was for CVLP (downstream of AMMC). We conjecture that the function of CVLP is not limited solely to a second-layer center of the auditory/mechanical modality.

Polarities of most of the heavily connected LPUs, like DMP, VMP, VLP-D, SDFP, and CVLP, were close to zero. These versatile nodes simultaneously act as both senders and receivers.

Edge Polarity

Most edges between LPUs are bi-directional, and approximately 15% of them are uni-directional (defined as edge polarity >0.9) (Figure S3A). The ratio for *C. elegans* and macaque are 53% [13] and 20% [14], respectively.

Betweenness Centrality, $\vec{b}$

The betweenness centrality of a node is the number of shortest paths between pairs of other nodes passing through the original node (Figure 1C). This term measures the node's relative importance in the efficient flow of information.

As expected, heavily connected nodes also had higher betweenness centralities. The Pearson's correlation between strength and betweenness of nodes was $\rho(\vec{s}, \vec{b}) = 0.817$. However, the exceptions were more interesting, e.g., the betweenness ranks of lobula (LOB and lob), 10th and 8th, respectively, were much higher than their ranks in strength (26th and 17th). This finding suggests that LOB and lob are more important in passing information than expected based on their moderate node strength. Similarly, the betweenness ranks of LH and lh (19th and 13th) were also higher than expected from their strengths (27th and 24th).

Global Centrality

Besides strength and betweenness, five other types of centralities were measured: degree, vulnerability, page rank, closeness, and dynamical importance (Figures 1D and S3). For each type of centrality, the top 12 out of 49 nodes (top quartile) earned 1 point. The total number of points collected by each node from the seven centralities was defined as its global centrality. Nodes with high global centrality correspond to network hubs.

Edge Betweenness

Edge betweenness is a measure of the importance of each edge in efficient communication (Figure S4A). The top five edges with highest betweenness were (FB → dmp), (SDFP → FB), (sdfp → FB), (FB → DMP), and (lob → vlp-d).

Strength Distribution

The data indicate the presence of a broad range of node strengths (black bars), clearly distinguishable from the more sharply peaked distribution (gray bars) in the randomized network (Figure 1E).

Small-World Characteristics

Small-world attributes were tested for the network (Figure 1F) [15]. The small size of the LPU network (49 nodes) and the large number of pathways (80% of all possible pathways contained at least one fiber) limited the level of small-world attributes. Thresholding was performed on the structural connection matrix by gradual removal of the weakest pathways (which may also be regarded as potential false positives) from the analysis. Retention of stronger pathways tended to boost normalized clustering

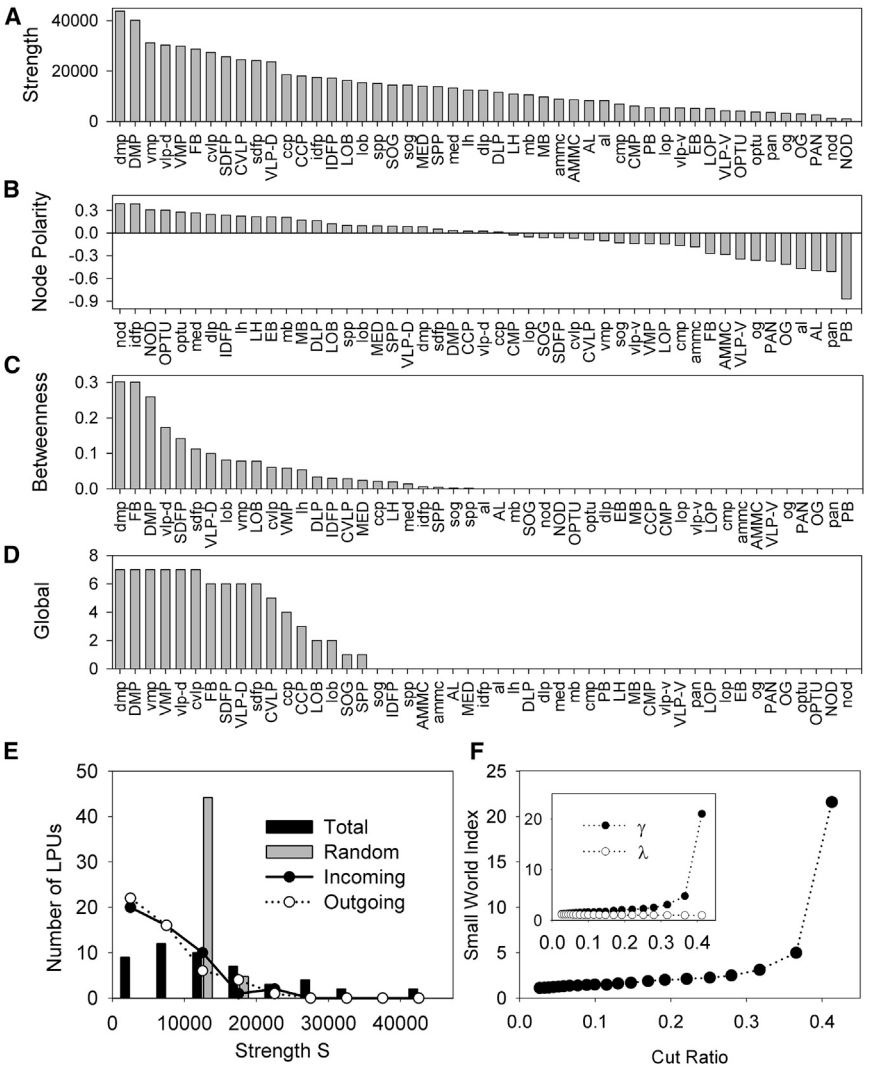

Figure 1. Basic Measurements for the Directed Brain Network

(A–D) Sorted total strength (A), node polarity (B), betweenness centrality (C), and global centrality (D) of the nodes. Other centralities can be found in Figure S3.

(E) Distribution of the total (black bars), incoming (filled circles), and outgoing (empty circles) strengths. Gray bars show the distribution for the network by randomly assigning the LPUs innervated by the fibers (averaged from 1,000 realizations; error bars are smaller than the border line of the gray bars).

(F) Small-world index versus the cut ratio, which is defined as the ratio between the total strength of the removed weakest links divided by the sum of the strengths of all links. For example, a cut ratio of 0.2 corresponds to a removal of 20% of the total link weights. Inset: normalized clustering coefficient (filled circles) and normalized path lengths (open circles).

See also Figures S1, S2, S3, and S10.

while leaving the normalized path length unaffected, and hence revealed stronger small-world attributes.

Modular Structure

The brain network can be divided into five functional modules by maximizing modularity [16]. The modular structure and connectivity matrix are shown in Figures 2A and S4B, respectively. Four of the five modules corresponded to sensory modalities—olfaction (containing the known LPUs AL, MB, and LH), auditory and mechanosensation (containing CVLP and AMMC), and bilateral areas for vision (containing MED). The central complex module, composed of the LPUs FB, ellipsoid body (EB), PB, IDFP, and noduli (NOD), is the integration center for visuo-locomotor behaviors in all arthropods [17, 18] and is important for decision making and locomotor output [19–23]. Given its known functions and intensive connections with the sensory modules, we refer to it as the "pre-motor" center.

Based on the within-module strengths, z, and participation coefficients, P, of the nodes in Figure S4C, we identified the central node for each functional module and the main connectors between modules [24]. The central nodes SDFP, DMP, LOB, and FB had the highest within-module strengths for olfactory, auditory, visual, and pre-motor centers, respectively. Superpenduncular protocerebrum (SPP; olfactory), DMP (auditory), VLP-D (visual), and IDFP (pre-motor) had the highest normalized participation coefficients in their modules, implying that they were the inter-modular connectors. The main connectors between module pairs are listed in Document S2.

Sub-modular Structures of Olfactory and Auditory Modules

A hierarchical modular structure of the brain was reflected in our finding that the olfactory and auditory centers had sub-modular structures (shown in Figured 2B and 2C) when inter-modular connections were removed. The olfactory module consisted of four sub-modules, two of which (yellow and purple in Figure 2B) were the outermost sensory inputs on each side. One unidirectional pathway (defined as having a minimal but non-zero link in the reverse direction), AL→LH→DLP, was even stronger than the well-known AL→MB pathway. Furthermore, this analysis revealed that DLP integrated information from LH, SPP, and SOG, which then communicated with SDFP. These findings suggest that this pathway deserves more attention for understanding olfactory computation in the fly brain. The sub-module of green nodes, MB and SDFP of both hemispheres, formed the core for olfactory signal processing. MB and SDFP also received signals from AL and DLP, respectively. The four LPUs in this core were densely connected to each other. The last sub-module (shown in red) was the bilateral SOG. The SOG communicated mainly with SDFP, but also sent feedback signals to SPP and DLP. Finally, the major decussate connections in the olfactory module were SDFP→mb, sdfp→MB, SDFP↔sog, and sdfp↔SOG, and these connections help to form more loops,

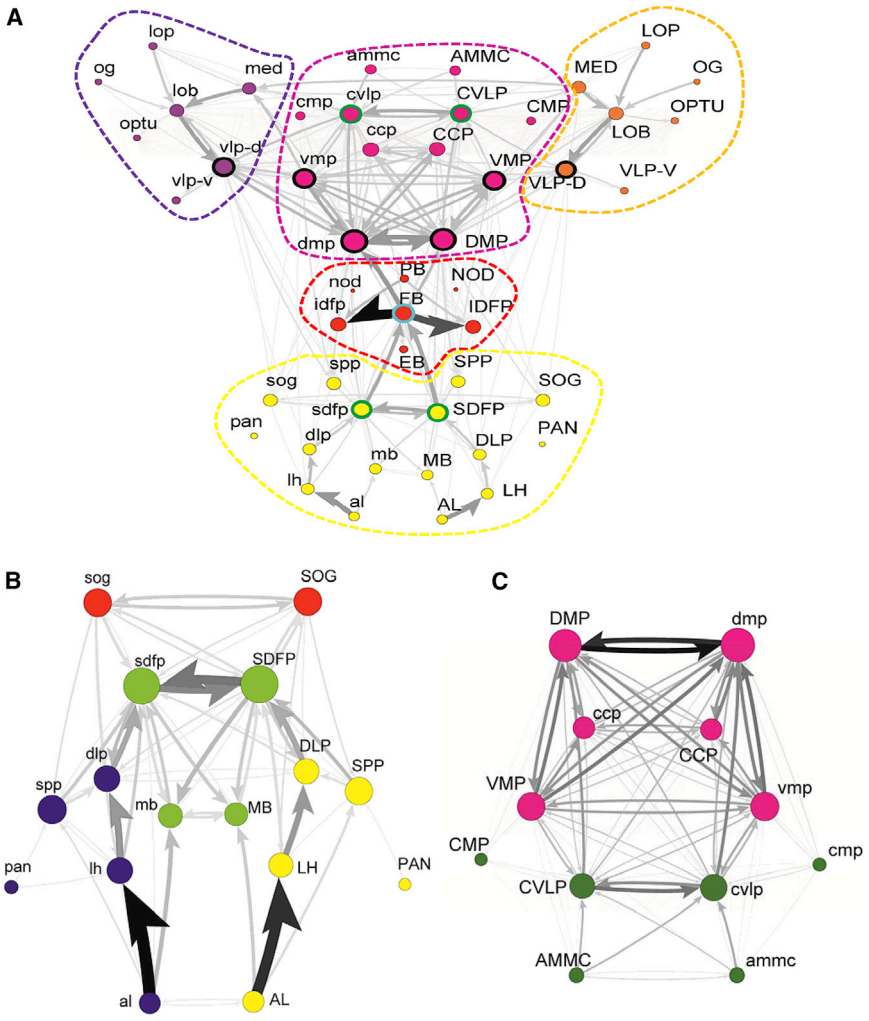

Figure 2. Modular Structure of the *Drosophila* Brain

There are five modules in the brain network: olfaction (yellow), auditory/mechanosensation (magenta), right vision (orange), left vision (purple), and pre-motor (red) (A). The LPUs with thick black and green boundaries indicate the innermost and second innermost rich-club members, respectively. Node size is proportional to the strength of the LPU. Arrows denote the direction of the connections. Darker and thicker lines represent stronger connections; (B) and (C) show the sub-modular structures of olfactory and auditory modules, respectively. See also Figure S4.

whose significance for signal processing warrants further investigation.

The three major modalities differed in their degree of left-right separation, from the most segregated (vision) to the least segregated (auditory). For example, left and right visual inputs were completely separated into different modules. The olfactory system AL sent signals to MB and LH in the same hemisphere and was thus only separated into sub-modules. On the other hand, auditory module LPUs (magenta in Figure 2C) formed a very strongly interconnected core. The sub-structure of this module could be divided into two parts—auditory and mechanosensory input (green nodes, including AMMC, CVLP, and CMP) and the processing core (other nodes in magenta). AMMC projected bilaterally to both CVLPs, and caudalcentral protocerebrum (CCP) was observed to connect to LPUs in the opposite hemisphere even more densely than on the same side, implying that CCPs are involved in the comparison and analysis of signals from different directions.

DMP and VMP LPUs in the auditory core, together with the CVLP, also exhibited strong connections to LPUs in other modules, suggesting that they have functions beyond auditory signal processing. Further analysis showed that these nodes, together with VLP-D (vision) and SDFP (olfaction), formed a "rich club" (RC) thus making them candidates for the motor center of the brain (see below).

Rich Club

An RC is a set of high-strength nodes that are more densely connected with each other than expected with reference to an appropriate null model [25], and RCs have been found in brain networks of humans, macaques, and birds [26, 27]. We detected RC organization with multiple nested shells in the fly brain (Figure S4D). The RC member nodes in the three innermost shells were DMP, VMP, VLP-D, and SDFP for both hemispheres and FB in the central brain, most of which lie deep in the central brain. By definition, the links between RC members exhibited high edge betweenness.

Loops in the Brain

Signal transmission in the brain occurs on a scale of tens of milliseconds, and the small-world characteristics of the network imply that signal transmission time between any pair of LPUs will be hundreds of milliseconds. On the other hand, looped structures in the network would be capable of sustaining electrical signals for longer periods of time, and thus be important for recurrent circuits, such as those hypothesized for intermediate memory reverberation [28–30].

Traditional analyses of complex networks have focused on the properties of the shortest paths, which contain no loops, to address the efficiency of information transfer, or else examined looped structures statistically for the frequency of isomorphic network motifs [31]. Instead of this statistical approach, we have examined the strength and detailed structures of individual loops (Figure 3 and Figures S5–S7).

The two-loops (i.e., containing two LPUs) shown in Figures S5 and S6A were highly correlated with, but not identical to, tracts between LPUs (addressed in [4]). The two-loops were comprised

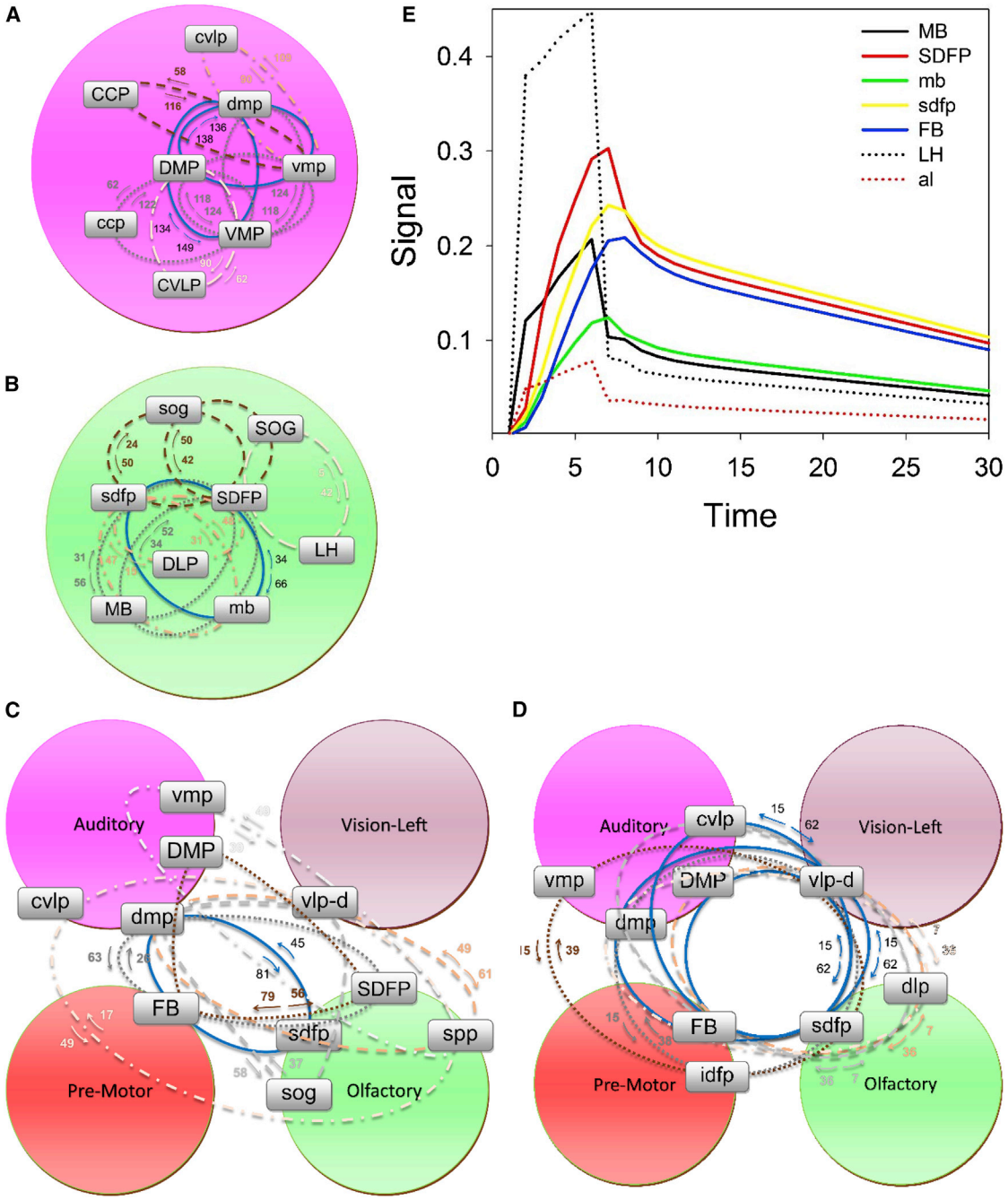

Figure 3. Major Loops in the Network

(A and B) Intra-modular LPU three-loops of the left auditory/mechanosensory module with loop strength >900 (at least for one direction) (A) and olfactory module with loop strength >420 (B).

(C) Three-loops connecting three modules with loop strength >490.

(D) LPU four-loops connecting four modules with loop strength >360. Note that the numbers in the figure (and in Figures S5–S7) are the loop strength divided by 10.

(A–D) Due to the hemispherical symmetry, only the left visual module is shown in (C) and (D). Some loops are only shown in one hemisphere in the figures. For example, although only the dmp ⇄ vmp ⇄ CCP ⇄ dmp loop in the left brain is shown in (A), the symmetric loop DMP ⇄ VMP ⇄ ccp ⇄ DMP in the left brain exists, although it is not shown in the figure. This was done to reduce the complication of figures. More detailed information for the loops can be found in Figures S5–S7. For clarity, only one (left) of the two visual modules is shown in these figures.

(E) The persistence of the olfactory signal injected to AL and sent out to the body from DMP and dmp.

See also Figures S5–S7.

of bi-directional connections between the LPUs, whereas tracts could be uni- or bi-directional.

Some three- and four-loops could be predicted from the two-loops. For example, the bi-directional LOB↔LOP↔MED↔LOB loop depicted in Figure S5B could be reduced to the three two-loops in the left part of Figure S5A. In contrast, the existence of irreducible loops implies a more complicated function that requires re-iteration or reverberation of information among more brain regions. Such irreducible long loops were found to be unidirectional and have large "loop polarity." For example, dmp↔CVLP and dmp↔FB were both strong two-loops (Figures S5D and S6A), but FB→CVLP was unidirectional. As a result, FB→CVLP→dmp→FB became a unidirectional loop with a polarity of 3.32 (Figure S6B).

The strongest three-loop (composed of three LPUs) in the olfactory module was the grouping mb↔sdfp↔SDFP↔mb ($\bar{\ell}=1.94$, Figure 3B), whereas in the auditory module it was VMP↔dmp↔DMP↔VMP ($\bar{\ell}=1.11$, Figure 3A). All three of the nodes were RC members.

Figure 3C shows multiple three-loops that connect three modules. The strongest of these was dmp↔sdfp↔FB↔dmp ($\bar{\ell}=1.8$), which connects the auditory, olfactory, and pre-motor modules.

Figure 3D shows the four-loops connecting four different modules, of which the strongest was DMP→vlp-d→sdfp→FB→DMP. It was also strongly polarized ($\bar{\ell}=3.95$).

In general, intra-modular loops were stronger than inter-modular loops, and shorter loops were stronger than longer ones. Further studies will be needed to address the function of these loops. One possibility is that they allow signals to persist in the brain over short to medium timescales, such as those involved in the early stages of memory formation.

In order to test this idea, we simulated the persistence of an olfactory signal. A signal injected into the AL from time steps t = 1–3 propagated in the network until t = 30 according to the connectivity matrix. A portion of the signals were exported as motor output from the DMP and dmp (see the Supplemental Experimental Procedures). The resulting signal strength versus time for several LPUs is shown in Figure 3E. SDFP, sdfp, and FB had the strongest responses for an olfactory stimulus. In contrast, signals in MB and mb were less persistent but were still stronger than that in LH, which was the strongest downstream LPU of the AL. Signal strength in the SDFP and FB persisted for one to three time steps after the input stopped. On the other hand, signals in LH and al, the counterpart of the AL in the left hemisphere and immediately downstream from AL, decayed quickly after the input ceased. The persistence of the signal in SDFP, sdfp, and FB was a consequence of the strong loop structure discussed above. In contrast, the rapid decay of the signal in the LH was due to a lack of loops.

Information Flow during Behavior

As discussed previously, the dense intra- and inter-modular connectedness of the core of the auditory module suggests that it has more functions than just processing auditory signals. RC members DMP and VLP-D were found to be heavily innervated by dendrites of the giant fiber neurons (Figure S8) descending from the brain into the thoracic ganglion and critical for the fly's escape response. This suggests that DMP and VLP-D pairs are the main gateways that send motor action commands. Another LPU, SOG, although not part of the RC, received its main signals from RC members DMP, SDFP, and VMP and projected down to the thoracic ganglion. This implies that the RC→SOG pathway is an alternative or parallel information channel from sensory input to motor output.

Aside from innervating the giant fiber, DMP and VLP-D had the highest scores in nearly all measurements of centrality. Furthermore, they were the innermost members of the RC. According to the overall structure of connections discussed above, we conjecture that the RC members form the motor center in the *Drosophila* brain (black square in Figure 4), which may be the hypothesized second function of the auditory module.

Figure S9A shows the inter-modular connections of the network. The auditory module was heavily connected to all other modules, with the auditory-olfactory connection being the strongest. We deconstructed these super-modular connections into two types, as shown in Figure S9B. The first type of connection directly joined the motor center and sensory input modules (black and gray arrows), whereas the second type formed loops among olfactory, pre-motor, and motor centers (red arrows).

Based on Figure S9B, together with the RC and loop structures discussed above, possible pathways of information flow for different types of *Drosophila* behaviors are summarized in Figure 4.

ACh/GABA Network

The foregoing discussions of connectivity did not distinguish between excitation and inhibition. Since the imaged neurons in *FlyCircuit* were labeled using genetic drivers based on neurotransmitter synthetic enzymes and one vesicle transporter, we can predict their transmitter identity with reasonable certainty. For this initial treatment, we focused on the two major neurotransmitters in the fly brain, acetylcholine (ACh) and GABA, where ACh is generally excitatory and GABA inhibitory. The resulting network was based on 3,377 putatively cholinergic and 3,632 putatively GABAergic neurons.

First, we focused on the intra-modular connections of the two neurotransmitters for the five modules shown in Figure 5A. The net strength of the edges shown in this network was defined as $s_{ij}^{net}=s_{ij}^{e}-s_{ij}^{i}$, where s_{ij}^{e} and s_{ij}^{i} describe the excitatory and inhibitory strength of the link directed from i^{th} to j^{th} node. Red links represent positive net strength (i.e., stronger excitatory features), and black links exhibit negative net strength (i.e., inhibitory).

The strongest intra-modular inhibition occurred in the pre-motor module. Specifically, we found that PB inhibited the FB and IDFP pair and that FB also inhibited the IDFP pair. Inhibition of this region could reduce noise and could balance excitation in order to avoid seizure-like activity.

In the sensory modalities, the main visual input, MED, and the center of the module, LOB, both appeared to be mutually excited. In contrast, the main olfactory input, AL, was found to send more inhibitory connections to MB and LH, which may be related to the combinatorial mechanism of odor coding [32]. The strength of excitatory and inhibitory links from the AMMC, the main auditory input, to CVLP was comparable. Thus, the three main sensory modalities exhibited different excitatory/inhibitory ratios.

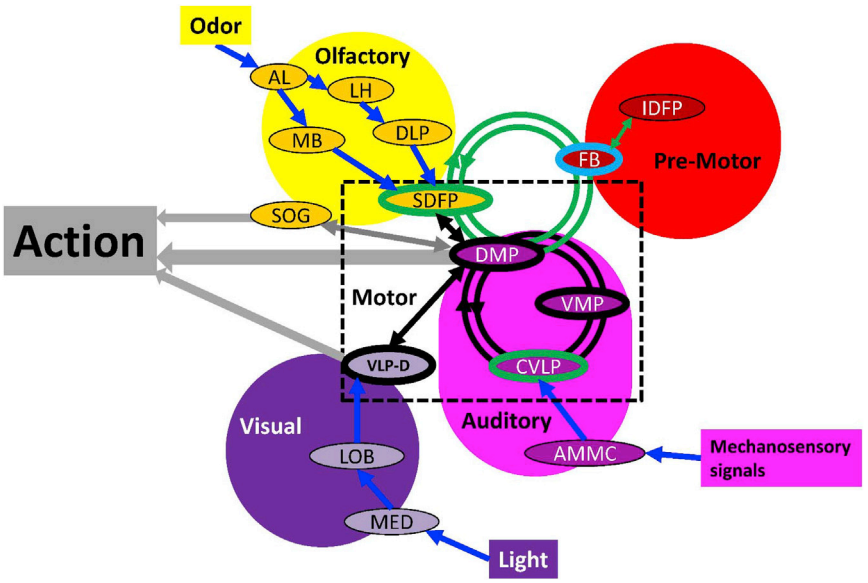

Figure 4. Information Flow during Behaviors
Sensory stimuli for different modalities acted on first layer LPUs: AL for olfactory, AMMC for auditory, and MED for visual signals. Stimuli were then processed in their corresponding sensory modules along the pathway indicated by the blue arrows. Signals then converged on RC (motor center) members in their respective modules: SDFP, VLP-D, and CVLP for olfactory, visual, and auditory signals, respectively. After processing in the motor center (black arrows), output commands were sent mainly through DMP and VLP-D, or alternatively via RC→SOG. The motor center communicated with the pre-motor center, and involved the SDFP↔FB↔DMP (indicated by green circles), which was the strongest three-loop that connected three modules (Figure 3C). The motor center was composed of edges with highest edge betweenness (Figure S4A). Taken together, these data suggest that decision-making is processed through an alternative pathway after a certain amount of reiteration between the pre-motor and motor centers. The motor center then launches a command of actions according to that decision. See also Figures S8 and S9.

Inter-modular connections for s_{ij}^{net} are shown in Figure 5B. FB and PB (pre-motor) displayed the greatest inhibition of DMP and CVLP pairs. Moreover, the VLP-D (visual) exhibited more excitatory-type communication with olfactory and auditory modules.

DISCUSSION

We present a first draft of a mesoscopic connectome of the *Drosophila* brain and perform a quantitative analysis of the directed, weighted network formed by LPUs and their connections. Modularity analysis showed that the network could be organized into five modules, including four sensory modality centers: olfaction, auditory/mechanosensory, vision (left and right), and the pre-motor center of the central brain. Furthermore, we determined that an RC, whose members were located in auditory and olfactory modules, occupied the role of the sensorimotor integration center of the brain.

Our analysis revealed important patterns of connectivity and information flow and also points to the importance of considering connection strengths for explaining function. Strong nodes and edges tend to dominate the results, but weak links, or nodes with low strength/betweenness centrality, could also play critical roles in brain functioning [33]. For example, the well-known importance of MB and EB was not highlighted in this analysis, which implies that connection strength per se may not be sufficient to evaluate the functional significance of LPUs and their connections. From an economic point of view, strong connections must be functionally important due to their large volume consumption and high metabolic cost in the maintenance of synapses and neurites. Thus, strong connections are necessary, but they may not be sufficient for indexing node importance. Ultimately, more detailed and activity-based methods will be necessary to gain a fuller picture of the brain [2].

Previous overviews of the insect brain have been based on compilations of classical anatomical findings. A classic review of the structure of arthropod brains [34] has only a small amount of connectivity information. Strausfeld's foundational fly brain atlas provided the first overall framework based on extensive staining of neural tracts, and it includes summaries of connection pathways among major brain regions, generally consistent with those presented in the current study [35]. Anatomical tracer studies in the cockroach were collected into a detailed connectivity diagram among brain regions and modalities in an effort to infer functional organization [36]. While generally consistent with our findings, these earlier studies could not quantify relative strengths of connectivity. More importantly, the organizational scheme was based only on morphologically recognizable structures. The current study employs a non-biased sampling of neurons followed by a non-biased parsing of neurons into LPUs, projection neurons, and connecting units [4]. The fact that the structures often correspond to anatomically recognizable brain areas is presumably not coincidental, but the analysis is more powerful for being based on connectivity criteria per se.

The availability of a complete network map for the brain of an invertebrate model organism invites comparisons to other such maps, including the nematode *C. elegans* [37, 38] and several vertebrate species [26, 27, 39]. Strikingly, several network attributes detected in the brain of *Drosophila* have analogs in the brains of other species, for example the existence of modules, interconnecting hubs, and a densely connected RC. A particularly intriguing comparison is with the network map of the rodent neocortex [40] This map resembles our fly scheme in the convergence of inputs from sensory modalities, visual and auditory in particular, into an interconnected set of structures—anterior cingulate (ACA), posterior parietal (PTL), and retrosplenial (RSP) cortical areas—that have extensive outputs to motor areas and an important role in motor decisions [41–43]. Thus, the ACA/PTL/RSP network may have genetic or further connectivity similarities to the fly auditory/mechanosensory/motor area and deserves further investigation. It may indicate the presence of

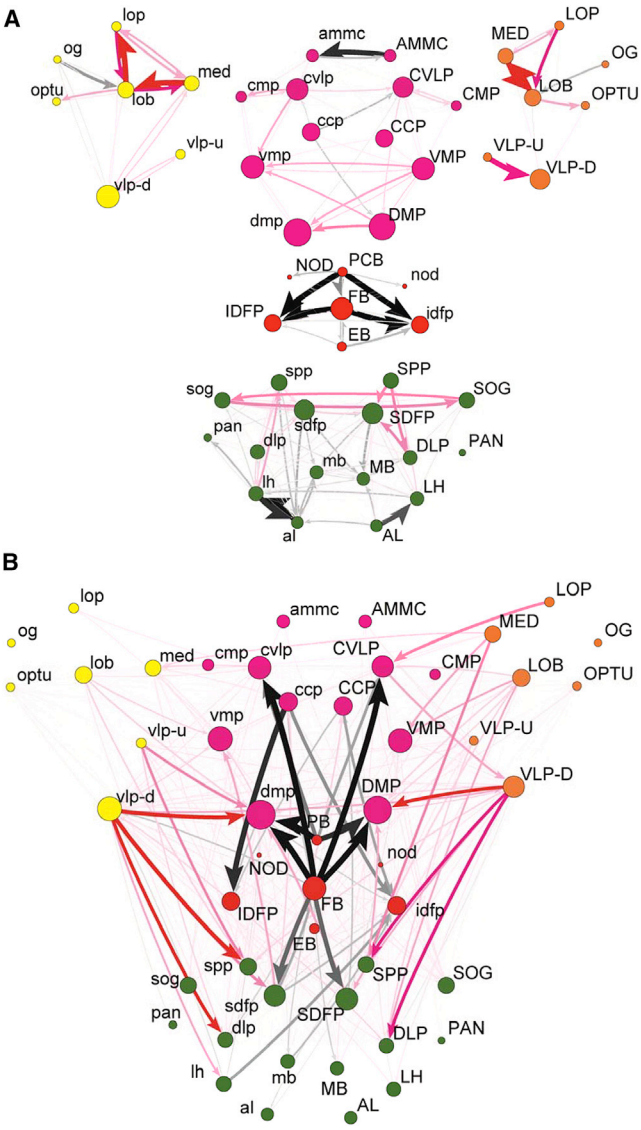

Figure 5. The Network of the Excitatory and Inhibitory Links

The intra-modular (A) and inter-modular (B) connections. The type (color) and strength (thickness) of the links were determined by the difference between the strength of the putative cholinergic (excitatory) and GABAergic (inhibitory) links. Red and black arrows represent stronger excitatory and inhibitory links, respectively. Node sizes are proportional to their total strength, as in Figure 2. Note the figure displays the difference between the strength of excitatory and inhibitory links; thus, original strengths are not shown. The behaviors of the two hemispheres are not symmetrical, possibly because the subtractive nature of s_{ij}^{net} caused large fluctuations of this value.

similar overall strategies of brain organization across distant phyla, already suggested by the similarities between central complex and basal ganglia [18, 44].

Assuming that fly brain regions have counterparts in mammals, we would not expect a one-to-one correspondence. The mammalian brain has been elaborated into many more distinct regions than any arthropod brain [34, 45]. Therefore, it seems reasonable to consider that if the fly brain does indeed have some correspondence to that of mammals, a given brain region may embody properties that are subdivided into multiple regions in a mammal. In this instance, the correspondence would be between fly central complex and mammalian ACA, PTL, and RSP cortical areas, as well as basal ganglia. The relevant interconnections among these regions, ACA, PTL, and RSP [40], and basal ganglia [46–48], have all been demonstrated.

From both evolutionary and engineering perspectives, the apparent common organization across phyla may simply be part of a necessary logic. Information from sensory systems needs to be integrated so that appropriately adaptive decisions and plans can be made and executed as motor outputs. If this integration requires any computational complexity, as it undoubtedly does, then it needs to converge into a suitably complex network for those computations to be made.

EXPERIMENTAL PROCEDURES

FlyCircuit: The Neuronal Image Database

23,579 single neurons were imaged and categorized according to their drivers, updating the collection [4] and including 18,179 neurons from females and 5,400 neurons from males (Table 1). Female neurons were divided into 3,355 local neurons and 14,824 projection neurons. Each neuron with its soma was confirmed and set as the initial point for tracing its skeleton with an algorithm modified from [49].

Classification of Neuron Polarity

The polarity of each structural domain was classified using the skeleton-based polarity identification for neurons (SPIN) method [5–8]. The complete list of neuron polarities can be found in the supplemental spreadsheet file "connectivity_polarity.xlsx."

Network Construction

The position of the dendrite of i^{th} neuron was located at the LPU D_j with terminal number d_i, and the axons at LPU X_i, with terminal number x_i, then $A^{(i)}_{D_j X_i} = \sqrt{d_i x_i}$. $A^{(i)}_{j,k} = 0$ otherwise. $A^{(i)}$ was an $N_U \times N_U$ matrix for each neuron. The matrix representation of the connectome was $A = \sum_{i=1}^{i=N_n} A^{(i)}$. $N_n = 12995$ and $N_U = 49$ were the number of neurons and the number of LPUs, respectively. The complete list of the connectivity matrix can be found in Document S2.

Network Measurements

Standard measurements in the complex network theory were performed on the *Drosophila* brain network mostly with the Brain Connectivity Toolbox [50]. Details for the measurements can be found in the Supplemental Experimental Procedures.

SUPPLEMENTAL INFORMATION

Supplemental Information includes Supplemental Experimental Procedures, ten figures, two tables, and predicted polarities and connectivity matrix and can be found with this article online at http://dx.doi.org/10.1016/j.cub.2015.03.021.

ACKNOWLEDGMENTS

We are grateful to the National Center for High-Performance Computing in Taiwan for their assistance in computation and by grants from the National Science Council in Taiwan to C.-T.S. (NSC-100-2112-M-029-001-MY3) and to C.-C.L. and T.-S.S. (NSC-101-2311-B-007-008-MY3), from the Ministry of Science and Technology in Taiwan to A.-S.C. (MOST-103-2633-B-007-001) and to C.-C.C. (MOST-103-2221-E-492-023), from the NSF (CIF-BCSP-1212778) to A.-S.C., O.S., and R.J.G., and from the Mathers Foundation to A.-S.C. and R.J.G. This work was supported by the Ministry of Science and Technology and the Ministry of Education in Taiwan.

Received: November 12, 2014
Revised: March 5, 2015
Accepted: March 13, 2015
Published: April 9, 2015

REFERENCES

1. Sporns, O., Tononi, G., and Kötter, R. (2005). The human connectome: A structural description of the human brain. PLoS Comput. Biol. *1*, e42.
2. Alivisatos, A.P., Chun, M., Church, G.M., Deisseroth, K., Donoghue, J.P., Greenspan, R.J., McEuen, P.L., Roukes, M.L., Sejnowski, T.J., Weiss, P.S., and Yuste, R. (2013). Neuroscience. The brain activity map. Science *339*, 1284–1285.
3. Bullmore, E., and Sporns, O. (2009). Complex brain networks: graph theoretical analysis of structural and functional systems. Nat. Rev. Neurosci. *10*, 186–198.
4. Chiang, A.S., Lin, C.Y., Chuang, C.C., Chang, H.M., Hsieh, C.H., Yeh, C.W., Shih, C.T., Wu, J.J., Wang, G.T., Chen, Y.C., et al. (2011). Three-dimensional reconstruction of brain-wide wiring networks in Drosophila at single-cell resolution. Curr. Biol. *21*, 1–11.
5. Cuntz, H., Forstner, F., Haag, J., and Borst, A. (2008). The morphological identity of insect dendrites. PLoS Comput. Biol. *4*, e1000251.
6. Cuntz, H., Forstner, F., Borst, A., and Häusser, M. (2010). One rule to grow them all: a general theory of neuronal branching and its practical application. PLoS Comput. Biol. *6*, e1000877.
7. Rolls, M.M. (2011). Neuronal polarity in Drosophila: sorting out axons and dendrites. Dev. Neurobiol. *71*, 419–429.
8. Lee, Y.H., Lin, Y.N., Chuang, C.C., and Lo, C.C. (2014). SPIN: a method of skeleton-based polarity identification for neurons. Neuroinformatics *12*, 487–507.
9. Vosshall, L.B., Wong, A.M., and Axel, R. (2000). An olfactory sensory map in the fly brain. Cell *102*, 147–159.
10. Kamikouchi, A., Shimada, T., and Ito, K. (2006). Comprehensive classification of the auditory sensory projections in the brain of the fruit fly Drosophila melanogaster. J. Comp. Neurol. *499*, 317–356.
11. Lai, J.S., Lo, S.J., Dickson, B.J., and Chiang, A.S. (2012). Auditory circuit in the Drosophila brain. Proc. Natl. Acad. Sci. USA *109*, 2607–2612.
12. Morante, J., and Desplan, C. (2008). The color-vision circuit in the medulla of Drosophila. Curr. Biol. *18*, 553–565.
13. Kim, J.S., and Kaiser, M. (2014). From Caenorhabditis elegans to the human connectome: a specific modular organization increases metabolic, functional and developmental efficiency. Philos. Trans. R. Soc. Lond. B Biol. Sci. *369*, 20130529.
14. Felleman, D.J., and Van Essen, D.C. (1991). Distributed hierarchical processing in the primate cerebral cortex. Cereb. Cortex *1*, 1–47.
15. Watts, R.G., Huang, C., Young, M.R., Li, J.J., Dong, Z., Pennie, W.D., and Colburn, N.H. (1998). Expression of dominant negative Erk2 inhibits AP-1 transactivation and neoplastic transformation. Oncogene *17*, 3493–3498.
16. Newman, M.E.J. (2006). Modularity and community structure in networks. Proc. Natl. Acad. Sci. USA *103*, 8577–8582.
17. Homberg, U. (2008). Evolution of the central complex in the arthropod brain with respect to the visual system. Arthropod Struct. Dev. *37*, 347–362.
18. Lin, C.Y., Chuang, C.C., Hua, T.E., Chen, C.C., Dickson, B.J., Greenspan, R.J., and Chiang, A.S. (2013). A comprehensive wiring diagram of the protocerebral bridge for visual information processing in the Drosophila brain. Cell Rep. *3*, 1739–1753.
19. Homberg, U. (1987). Structure and function of the central complex in insects. In Arthropod Brain: Its Evolution, Development, Structure and Functions, A.P. Gupta, ed. (New York: Wiley), pp. 347–367.
20. Strauss, R., and Heisenberg, M. (1993). A higher control center of locomotor behavior in the Drosophila brain. J. Neurosci. *13*, 1852–1861.
21. Strausfeld, N.J. (1999). A brain region in insects that supervises walking. Prog. Brain Res. *123*, 273–284.
22. Strauss, R. (2002). The central complex and the genetic dissection of locomotor behaviour. Curr. Opin. Neurobiol. *12*, 633–638.
23. Wessnitzer, J., and Webb, B. (2006). Multimodal sensory integration in insects—towards insect brain control architectures. Bioinspir. Biomim. *1*, 63–75.
24. Guimerà, R., and Nunes Amaral, L.A. (2005). Functional cartography of complex metabolic networks. Nature *433*, 895–900.
25. Colizza, V., Flammini, A., Serrano, M.A., and Vespignani, A. (2006). Detecting rich-club ordering in complex networks. Nat. Phys. *2*, 110–115.
26. Shanahan, M., Bingman, V.P., Shimizu, T., Wild, M., and Güntürkün, O. (2013). Large-scale network organization in the avian forebrain: a connectivity matrix and theoretical analysis. Front. Comput. Neurosci. *7*, 89.
27. Harriger, L., van den Heuvel, M.P., and Sporns, O. (2012). Rich club organization of macaque cerebral cortex and its role in network communication. PLoS ONE *7*, e46497.
28. Wu, C.L., Shih, M.F.M., Lai, J.S.Y., Yang, H.T., Turner, G.C., Chen, L., and Chiang, A.S. (2011). Heterotypic gap junctions between two neurons in the drosophila brain are critical for memory. Curr. Biol. *21*, 848–854.
29. Krashes, M.J., Keene, A.C., Leung, B., Armstrong, J.D., and Waddell, S. (2007). Sequential use of mushroom body neuron subsets during drosophila odor memory processing. Neuron *53*, 103–115.
30. Dubnau, J., and Chiang, A.S. (2013). Systems memory consolidation in Drosophila. Curr. Opin. Neurobiol. *23*, 84–91.
31. Milo, R., Shen-Orr, S., Itzkovitz, S., Kashtan, N., Chklovskii, D., and Alon, U. (2002). Network motifs: simple building blocks of complex networks. Science *298*, 824–827.
32. Hallem, E.A., and Carlson, J.R. (2006). Coding of odors by a receptor repertoire. Cell *125*, 143–160.
33. Goulas, A., Schaefer, A., and Margulies, D.S. (2014). The strength of weak connections in the macaque cortico-cortical network. Brain Struct. Funct. Published online July 18, 2014. http://dx.doi.org/10.1007/s00429-014-0836-3.
34. Bullock, G., and Horridge, G.A. (1965). Structure and Function in the Nervous Systems of Invertebrates, *Volume 2*. (San Francisco: W.H. Freeman and Co.).
35. Strausfeld, N.J. (1976). Atlas of an Insect Brain. (Berlin: Springer-Verlag).
36. Mizunami, M., Yokohari, F., and Takahata, M. (2004). Further exploration into the adaptive design of the arthropod "microbrain": I. Sensory and memory-processing systems. Zoolog. Sci. *21*, 1141–1151.
37. Varshney, L.R., Chen, B.L., Paniagua, E., Hall, D.H., and Chklovskii, D.B. (2011). Structural properties of the Caenorhabditis elegans neuronal network. PLoS Comput. Biol. *7*, e1001066.
38. Towlson, E.K., Vértes, P.E., Ahnert, S.E., Schafer, W.R., and Bullmore, E.T. (2013). The rich club of the C. elegans neuronal connectome. J. Neurosci. *33*, 6380–6387.
39. de Reus, M.A., and van den Heuvel, M.P. (2013). Rich club organization and intermodule communication in the cat connectome. J. Neurosci. *33*, 12929–12939.
40. Zingg, B., Hintiryan, H., Gou, L., Song, M.Y., Bay, M., Bienkowski, M.S., Foster, N.N., Yamashita, S., Bowman, I., Toga, A.W., and Dong, H.W. (2014). Neural networks of the mouse neocortex. Cell *156*, 1096–1111.
41. Bush, G., Vogt, B.A., Holmes, J., Dale, A.M., Greve, D., Jenike, M.A., and Rosen, B.R. (2002). Dorsal anterior cingulate cortex: a role in reward-based decision making. Proc. Natl. Acad. Sci. USA *99*, 523–528.
42. Desmurget, M., Reilly, K.T., Richard, N., Szathmari, A., Mottolese, C., and Sirigu, A. (2009). Movement intention after parietal cortex stimulation in humans. Science *324*, 811–813.
43. Vann, S.D., Aggleton, J.P., and Maguire, E.A. (2009). What does the retrosplenial cortex do? Nat. Rev. Neurosci. *10*, 792–802.
44. Strausfeld, N.J., and Hirth, F. (2013). Deep homology of arthropod central complex and vertebrate basal ganglia. Science *340*, 157–161.

45. Strausfeld, N.J. (2012). Arthropod Brains: Evolution, Functional Elegance, and Historical Significance. (Cambridge: Harvard University Press).
46. Cavada, C., and Goldman-Rakic, P.S. (1991). Topographic segregation of corticostriatal projections from posterior parietal subdivisions in the macaque monkey. Neuroscience *42*, 683–696.
47. Kunishio, K., and Haber, S.N. (1994). Primate cingulostriatal projection: limbic striatal versus sensorimotor striatal input. J. Comp. Neurol. *350*, 337–356.
48. Yeterian, E.H., and Pandya, D.N. (1993). Striatal connections of the parietal association cortices in rhesus monkeys. J. Comp. Neurol. *332*, 175–197.
49. Lee, P.C., Ching, Y.T., Chang, H.M., and Chiang, A.S. (2008). A semi-automatic method for neuron centerline extraction in confocal microscopic image stack. In 5th IEEE International Symposium on Biomedical Imaging, pp. 959–962.
50. Rubinov, M., and Sporns, O. (2010). Complex network measures of brain connectivity: uses and interpretations. Neuroimage *52*, 1059–1069.

